Differential Scanning Calorimetry Study and Computer Modeling of $\beta \Rightarrow \alpha$ Phase Transformation in a Ti-6Al-4V Alloy

S. MALINOV, Z. GUO, W. SHA, and A. WILSON

The relationship between heat-treatment parameters and microstructure in titanium alloys has so far been mainly studied empirically, using characterization techniques such as microscopy. Calculation and modeling of the kinetics of phase transformation have not yet been widely used for these alloys. Differential scanning calorimetry (DSC) has been widely used for the study of a variety of phase transformations. There has been much work done on the calculation and modeling of the kinetics of phase transformations for different systems based on the results from DSC study. In the present work, the kinetics of the $\beta \Rightarrow \alpha$ transformation in a Ti-6Al-4V titanium alloy were studied using DSC, at continuous cooling conditions with constant cooling rates of 5 °C, 10 °C, 20 °C, 30 °C, 40 °C, and 50 °C/min. The results from calorimetry were then used to trace and model the transformation kinetics in continuous cooling conditions. Based on suitably interpreted DSC results, continuous cooling–transformation (CCT) diagrams were calculated with lines of isotransformed fraction. The kinetics of transformation were modeled using the Johnson–Mehl–Avrami (JMA) theory and by applying the "concept of additivity." The JMA kinetic parameters were derived. Good agreement between the calculated and experimental transformed fractions is demonstrated. Using the derived kinetic parameters, the $\beta \Rightarrow \alpha$ transformation in a Ti-6Al-4V alloy can be described for any cooling path and condition. An interpretation of the results from the point of view of activation energy for nucleation is also presented.

I. INTRODUCTION

OVER recent decades, many titanium-based materials have been developed for different applications. Titanium alloys are desirable and sometimes essential materials from a "materials selection" viewpoint, due to their very good combination of mechanical properties and corrosion and erosion resistance. It is widely understood that the mechanical properties of titanium alloys depend on the characteristics of the microstructure.[1–4] The type of phases present, grain size and grain shape, and morphology and distribution of the fine microstructure ($\alpha + \beta$ colonies) determine the properties and, therefore, the application of titanium alloys. The microstructure is formed during thermomechanical processing. It is, therefore, important to know the kinetics of the phase transformations taking place during different heat-treatment regimes, which would allow optimization of the processing parameters (temperature, time, and cooling rate) in order to achieve the desired microstructure. It must be pointed out, however, that the relationship between heat-treatment parameters and structure for titanium alloys has, so far, only been studied empirically. The calculation and modeling of the kinetics of phase transformation have not yet been widely used for titanium alloys. Limited work[5,6] has been done on the physical modeling of time-temperature-transformation (TTT) diagrams for Ti alloys based on the Johnson–Mehl–Avrami (JMA) theory.

Differential scanning calorimetry (DSC), on the other hand, has been widely used as an experimental technique for the study of a variety of phase transformations.[7–14] Much work has been done on the calculation and modeling of the kinetics of phase transformations for different systems, based on the results from calorimetric curves.

In this work, the results of a DSC study have been used to model the kinetics of the $\beta \Rightarrow \alpha$ phase transformation in one of the most commonly used titanium alloys, Ti-6Al-4V. The kinetics were investigated under continuous cooling conditions. The modeling was based on the application of the JMA theory[15–18] and was motivated by the desire to understand fundamental kinetic and thermodynamic parameters.

II. EXPERIMENTAL PROCEDURES

A commercial alloy, Timetal 6-4 (Ti-6Al-4V, provided by TIMET UK Ltd.), was used in the present work and had a chemical composition of 6.59 wt pct Al, 4.1 wt pct V, 0.18 wt pct Fe, <0.01 wt pct C, 20 ppm H, 50 ppm N, and 1900 ppm O.

The DSC measurements were performed using a Netzsch DSC-404 apparatus. The same apparatus was used in Reference 19 for the investigation of the phase evolution of Ti-6Al-4V during continuous heating. Before commencement of the measurements, the calorimeter was calibrated for temperature and sensitivity using the melting curves of pure In, Zn, Al, Ag, and Au. In order to avoid sample oxidation, the experiments were performed in a He flow (30 mL/min) after evacuating the working chamber three times to a vacuum level of 10^{-2} mbar. The purity of the He used was higher than 99.999 pct. The sample dimension was 3.5

S. MALINOV and Z. GUO, Research Assistants, and W. SHA, University Reader, are with the School of Civil Engineering, The Queen's University of Belfast, Belfast BT7 1NN, Northern Ireland, United Kingdom. A. WILSON, Metallurgist, is with the Quality and Technology Department, TIMET Ltd., Birmingham B6 7UR, United Kingdom.

Manuscript submitted February 11, 2000.

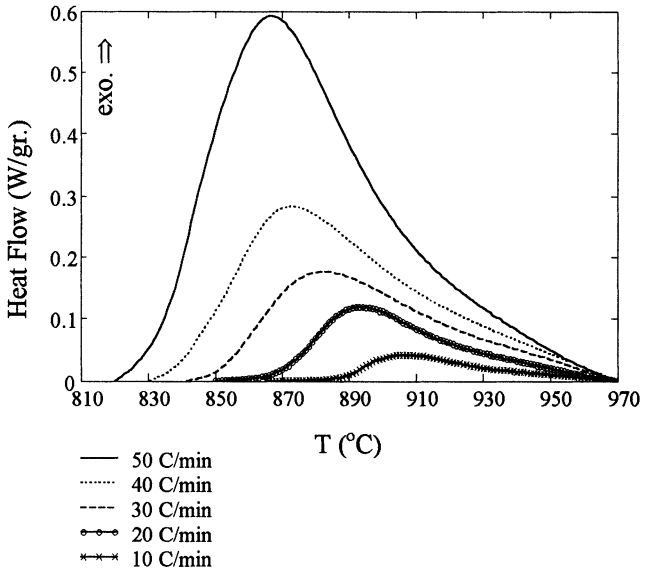

Fig. 1—Results from DSC runs for Ti-6Al-4V alloy employing different cooling rates.

× 3.5 × 2.3 mm, with a weight of 135 to 145 mg. Samples were placed in ceramic containers, and high-purity nickel was used as a reference material.

The DSC experiments were performed using the following time-temperature cycle: they were heated to 1100 °C (β field) using a heating rate of 20 °C/min, isothermally held at 1100 °C for 20 minutes, and thereafter cooled using varying cooling rates of 5 °C, 10 °C, 20 °C, 30 °C, 40 °C, and 50 °C/min. Two runs at each cooling rate were conducted. The first run was carried out using a Ni reference of identical mass in each pan in order to obtain a "baseline." The second run was performed by replacing the Ni reference in the sample pan with the Ti alloy of identical mass. The heat flow from the first run was automatically subtracted from the heat flow in the second, in order to obtain the heat flow due to the sample. Repeated DSC runs at each cooling rate were made to examine reproducibility, and this was found to be acceptable.

The phase constitution before and after DSC experiments was determined using X-ray diffraction. Measurements were performed at room temperature with a Siemens diffractometer, using Cu $K_{\alpha 1+\alpha 2}$ radiation from an angle of 32 to 75 deg (2θ), with a step size of 0.05 deg (2θ) and a counting time of 10 s/step.

The microstructure after different heat-treatment cycles was studied by optical microscopy, and image analysis was performed using LUCIA* software.

*LUCIA is a registered trademark of Laboratory Imaging, Ltd. The software is distributed by Nikon UK Ltd.

III. RESULTS AND DISCUSSION

A. *Interpretation of the DSC Measurements*

Figure 1 shows the processed DSC curves obtained from the different cooling rates. Each curve represents the average of three different runs using the same cooling rates and conditions.

It must be noted that, while the temperatures corresponding to the peak and the end of the transformation were clear and easily detectable, the temperatures corresponding to the start of the transformation were difficult to determine. As a result, a "best-fit" start temperature of 970 °C was used for all cooling curves. This assumption also agreed with the published continuous cooling–transformation (CCT) diagrams for the Ti-6Al-4V alloy.[20] According to the diagrams in Reference 20, the start temperature (970 °C) of the $\beta \Rightarrow \beta + \alpha$ transformation in continuous cooling is about the same for quite a large range of cooling rates (up to 200 °C/min). A similar result was obtained from the calculation of the incubation times for the cooling rates used, based on the isothermal incubation times and applying Scheil's sum.[21]

The DSC curves for all cooling rates had a similar asymmetry, with a "tail" at high temperatures (at the start of the transformation). The area under the curve from the start to the peak temperature ranged from 61 to 64 pct of the entire area from the start to the end temperature. Calculated enthalpies, as well as the other parameters of the DSC curves, are given in Table I.

It should be noted that the DSC results obtained disagreed with the published CCT diagram for Ti-6Al-4V[20]—specifically at the end of the $\beta \Rightarrow \beta + \alpha$ transformation. It was found that the end of the transformation was in the range from 820 °C to 865 °C, depending on the cooling rate (Table I), while for the same cooling rates, according to the CCT diagrams in Reference 20, the end of transformation was 670 °C to 690 °C. In order to clarify this discrepancy, additional experiments were carried out using an ordinary furnace with programmable heating/cooling rates. For a cooling rate of 20 °C/min, samples were taken out of the furnace from different temperatures (namely, 970 °C, 940 °C, 890 °C, 860 °C, 800 °C, and 750 °C) and water quenched. Thereafter, the degree of the transformation was traced using metallographic examination. It was found that the microstructure of the samples quenched from 970 °C, 940 °C, 890 °C, and 860 °C was $\alpha + \alpha'$ (martensite) (Figure 2(a)). The amount of α' naturally decreased with lower quenching temperatures. This implied that the β-phase transformation was incomplete. The microstructure of the samples quenched from 800 °C and 750 °C consisted of only acicular α phase (Figure 2(b)), implying that the transformation had been completed above 800 °C. From these results, it can be concluded that the end of the $\beta \Rightarrow \alpha + \beta$ transformation, at a cooling rate of 20 °C/min, occurred between 800 °C and 860 °C. This result confirmed the DSC results obtained, rather than the published CCT diagram.[20] However, the difference between the results in this work and those in Reference 20 might be due to the differences in the composition of the alloys used. It is well known that, for example, impurity or oxygen levels have a dramatic influence on the transformation kinetics.[22] Unfortunately, the oxygen level for the alloy used in Reference 20 was not given.

B. *Calculation of CCT Diagrams*

In similar DSC experiments by other authors,[9,13] it has been proposed that the degree of transformation is equal to the fraction of heat absorbed/released.

Table I. DSC Peak Parameters

Cooling Rate, °C/min	Start Temperature °C	Peak Temperature °C	End Temperature °C	Area from Start to Peak Temperature Pct	Enthalpy, J/g
10	970	908	865	61.4	24
20	970	894	850	62.2	25
30	970	883	841	63.6	26
40	970	873	830	63.7	27
50	970	867	820	62.4	*

*The cooling rate of 50 °C/min was too fast to allow accurate determination of the enthalpy.

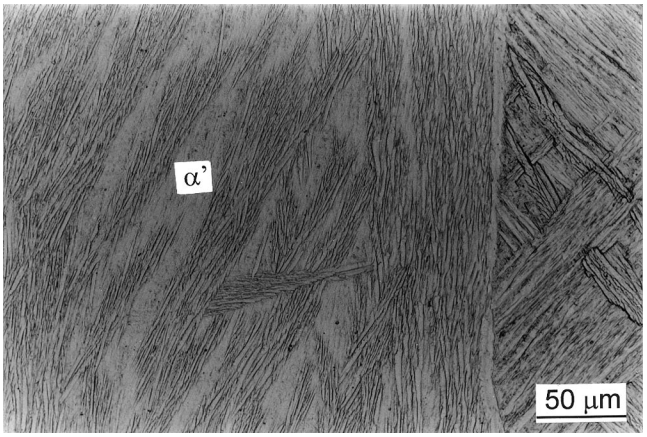

(*a*)

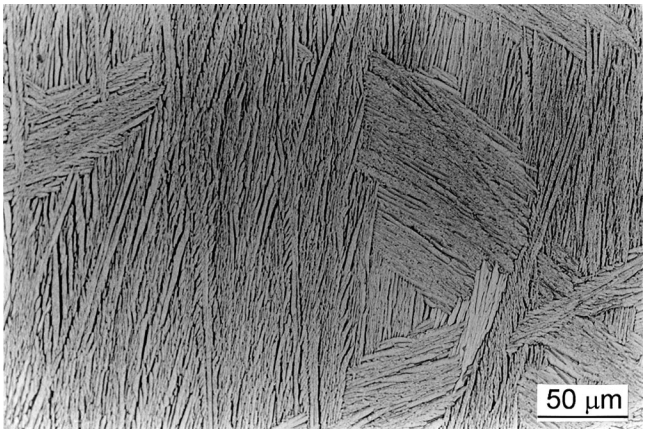

(*b*)

Fig. 2—Microstructure of Ti-6Al-4V alloy after continuous cooling with 20 °C/min and quenching from (*a*) 860 °C and (*b*) 750 °C.

$$f(t) = \frac{\int_{T_S}^{T} \frac{\partial h}{\partial t}\, dt}{\int_{T_S}^{T_E} \frac{\partial h}{\partial t}\, dt} = \frac{\int_{T_S}^{T} H dt}{\int_{T_S}^{T_E} H dt} \qquad [1]$$

where $\partial h/\partial t$ (H) is the heat flow measured, $f(t)$ is transformed fraction at any given time (t), and T_S and T_E are the transformation start and end temperatures, respectively.

Hence, from the DSC signal (Figure 1) and using Eq. [1], the degree of transformation as a function of the time or the temperature can be calculated and plotted. The calculated results for different cooling rates are presented in Figure 3.

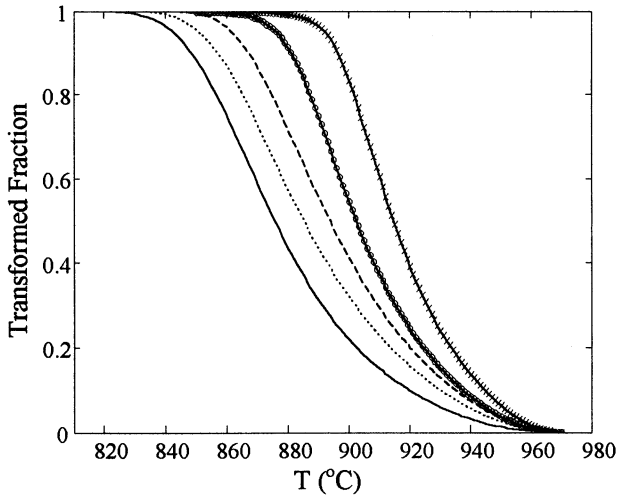

(*a*)

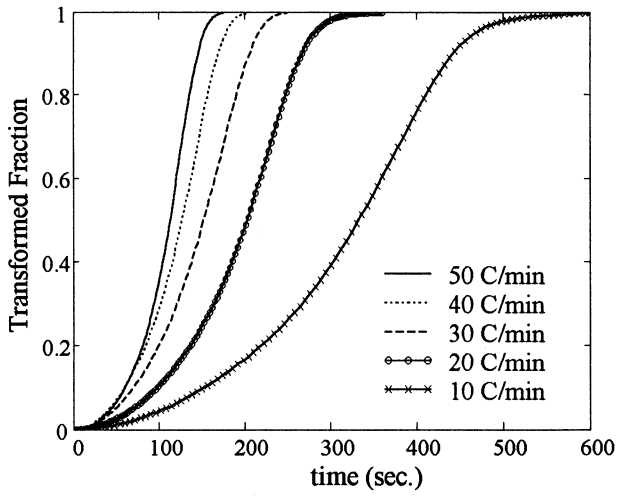

(*b*)

Fig. 3—Calculated transformed fraction as a function of the (*a*) temperature and (*b*) time for different cooling rates

The calculated curves labeled "Transformed fraction *vs* Temperature" and "Transformed fraction *vs* Time" (Figure 3) trace the course of the $\beta \Rightarrow \alpha$ transformation in the Ti-6Al-4V alloy. It must be emphasized, however, that for all cooling rates, a small amount of residual (or retained)

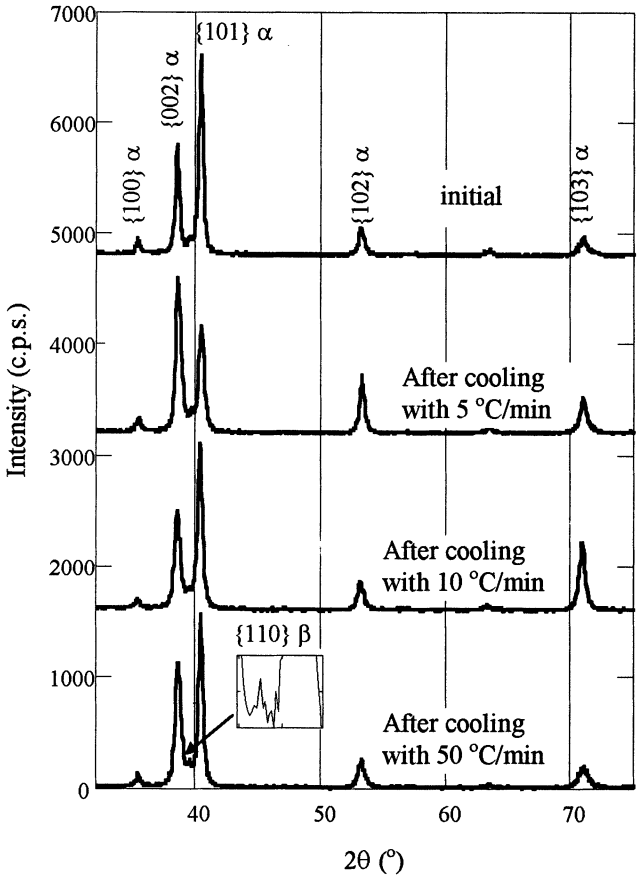

Fig. 4—X-ray diffraction patterns of Ti-6Al-4V samples after cooling with different rates. For clarity, the diffraction patterns are shifted along the vertical axis with respect to each other.

β remained after complete transformation (Figure 4). This amount was calculated from X-ray diffraction patterns using the "direct comparison method"[23] and was found to be 9 ± 2 wt pct. The amount of residual β is independent of the cooling rate. Therefore, for all cooling rates, the same phase transformation was traced (100 pct $\beta \Rightarrow$ 91 pct α + 9 pct β). The only difference between the X-ray diffraction patterns after different cooling rates was in the relative intensities of the different {h k l} planes of the α phase (Figure 4). This was probably due to "preferable orientations" of the α phase under different cooling rates.

Hence, hereafter in our calculations, a "100 pct" completed transformation corresponds to an actual phase composition of 91 pct α + 9 pct β. All calculations can very easily be converted from the "degree of transformation (from 0 to 100 pct)" to the "amount of α phase (from 0 to 91 pct)."

Applying Eq. [1] again for all the cooling rates used, the results are summarized in a contour plot (Figure 5) showing lines of "isotransformed fraction" as the temperature *vs* cooling rate. Such a thermokinetic diagram is a useful tool, since it can be used to trace the course of transformation in a real product, where the cooling rates in a (usually quite large) piece vary significantly from the surface to the core.

Finally, the calculated results are presented in the form of classical CCT diagrams (Figure 6). In these diagrams, isolines of equal transformed fraction for the different cooling rates are introduced. The CCT diagrams were calculated

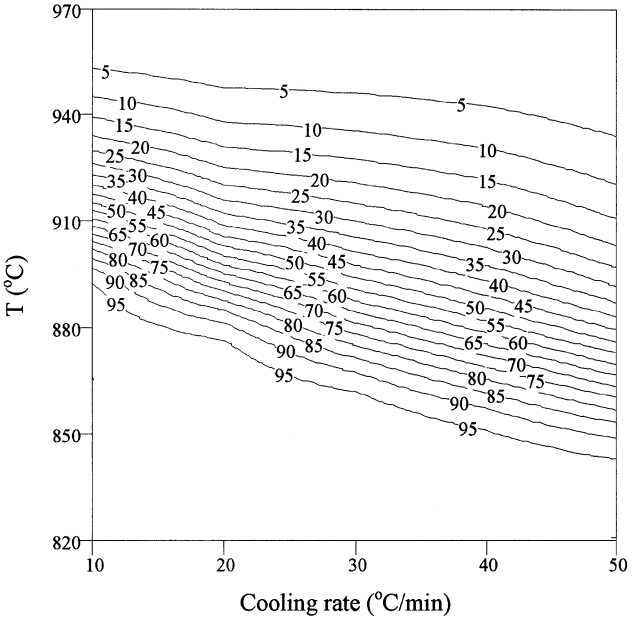

Fig. 5—Calculated thermokinetics diagram in temperature of transformation *vs* cooling rate. Isolines show the isotransformed fractions.

for two cases: (1) cooling from 1100 °C and (2) cooling from the β-transus temperature (1000 °C).

C. *Calculation of Transformation Kinetics*

The kinetics of isothermal transformations are usually expressed by the theory of transformation kinetics developed by JMA.[15–18] In its basic form, the theory describes the evolution of the volume fraction transformed with time:

$$f = 1 - \exp(-kt^n) \qquad [2]$$

where f is the product volume fraction, which varies with time t (in seconds); k is the reaction-rate constant; and n is the Avrami index.

In its general form, Eq. [2] applies to many real transformations. Under isothermal conditions, it describes a variety of phase transformations including polymorphic changes, discontinuous precipitation, eutectoid reactions, interface-controlled growth, diffusion-controlled growth, *etc*. However, it must be emphasised that Eq. [2] expresses JMA theory under the following assumptions:

(1) an isothermal transformation;
(2) a nucleation frequency that is either constant, or else is a maximum at the beginning of transformation and decreases during the course of transformation; and
(3) a spatially random nucleation.

There have been many attempts to adapt and use the previous theory for nonisothermal transformation.[24,25] In the past, the previous theory has been used as the theoretical basis for interpretation of differential thermal analysis (DTA) and DSC results.[8–14,26] Different methods (based on JMA theory) have been developed and used for describing the course of nonisothermal phase transformations and calculating kinetic parameters. Among them are the following.

(1) Direct integration of the generalized form of the JMA equation,[8]

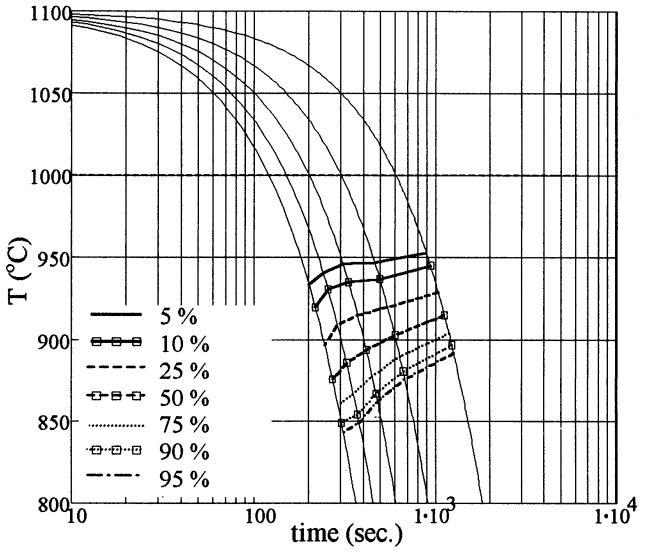

(*a*)

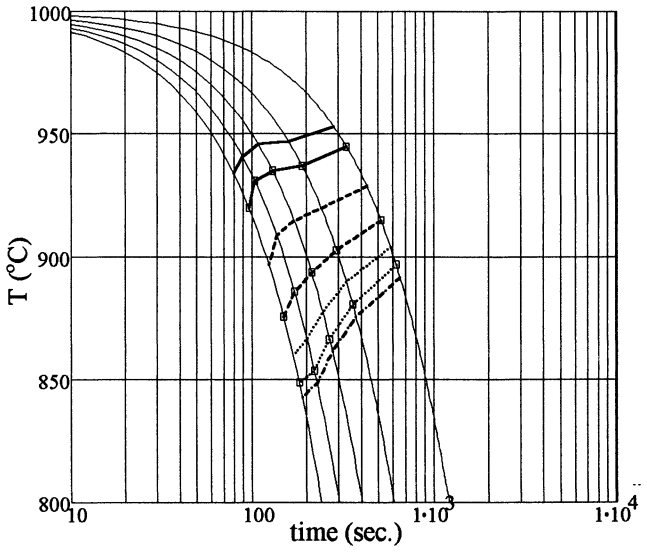

(*b*)

Fig. 6—CCT diagram of Ti-6Al-4V alloy for cooling from (*a*) 1100 °C and (*b*) 1000 °C (β-transus). The calculations are from DSC data. Isolines show the isotransformed fractions.

$$f = 1 - \exp\left(-g\int_0^t I_V\left(\int_0^{t'} u d\tau\right)^m dt'\right) \qquad [3]$$

where f is the transformed volume fraction at time t, I_V is the nucleation frequency, u is the growth rate, g is a geometrical factor, τ is an integrated variable, and $m = n - 1$.

(2) Introduction of new state variable,[9,11–13,24]

$$f = 1 - \exp(-\theta^n) \qquad [4a]$$

where f is the transformed volume fraction, n is the Avrami exponent, and

$$\theta = \int_0^t k(T)dT; \qquad k(T) = k_0 \exp\left(\frac{-Q}{RT}\right) \qquad [4b]$$

where k_0 is the pre-exponential factor, Q is the activation energy, and R is the gas constant.

In general, it can be summarized that all the previous models have been successfully applied to describe the kinetics of phase transformations during continuous heating and have been mostly used for the processes of crystallization of amorphous materials. This is a relatively simple case compared to the phase transformation taking place during continuous cooling, because during heating, both nucleation and growth rates increase constantly with temperature.

In situations where phase transformation takes place on cooling, the nucleation rate is determined by a Boltzman-type equation, which has an activation energy that decreases more than linearly with temperature.[27] This gives a rapidly increasing nucleation rate as the undercooling increases (the temperature decreases). The growth rate, in contrast, is controlled by an activation energy that is considered to be temperature independent, and, hence, the growth rate decreases as the undercooling increases (the temperature decreases). These opposing factors give an overall transformation rate.

Taking these into account, it can be concluded that the methods described for tracing the course of phase transformation during heating cannot be directly applied to the case of phase transformation during continuous cooling.[28] For this reason, in the present work, we replace continuous cooling with the sum of small, consecutive isothermal steps. This concept has been used in many works to study the kinetics of different phase transformation from DSC results. In the present work, we follow this approach to describe the kinetics of the $\beta \Rightarrow \alpha$ phase transformation during continuous cooling in a Ti-6Al-4V alloy.

The *T-t* path of continuous cooling is replaced by the sum of consecutive isothermal steps (Figure 7) at the temperatures T_1, T_2, and T_i (note that the cooling rate is a constant). For each isothermal stage, JMA theory for isothermal phase transformations (Eq. [2]) is applied. Hence, for cooling from point 0 to point 1, the following can be written:

$$f_1 = 1 - \exp(-k_1 \Delta t^{n_1}) \qquad [5a]$$

where f_1 is the transformed fraction from 0 to 1 (Figure 7), k_1 and n_1 are the JMA kinetics parameters at temperature T_1, and Δt is the isothermal time.

For tracing the transformation from points 0 to 2, the principle of additivity must be kept.[24,29–31] Therefore, the first fictitious time for point 1 is calculated using

$$t^*_2 = \sqrt[n_2]{\frac{\ln(1 - f_1)}{-k_2}} \qquad [5b]$$

where t^*_2 refers to the "time after which the amount f_1 would have been transformed if the whole transformation were at an isothermal temperature of T_2, with kinetics parameters of k_2 and n_2." Thereafter, the time is incremented by Δt, and, for the interval from points 0 to 2, one may write

$$f_2 = 1 - \exp(-k_2 \cdot (t^*_2 + \Delta t)^{n_2}) \qquad [5c]$$

From the previous reasoning, the general case for the interval from points 0 to i is as follows:

$$f_i = 1 - \exp(-k_i \cdot (t^*_i + \Delta t)^{n_i}) \qquad [5d]$$

where

$$t^*_i = \sqrt[n_i]{\frac{\ln(1 - f_{i-1})}{-k_i}} \qquad [5e]$$

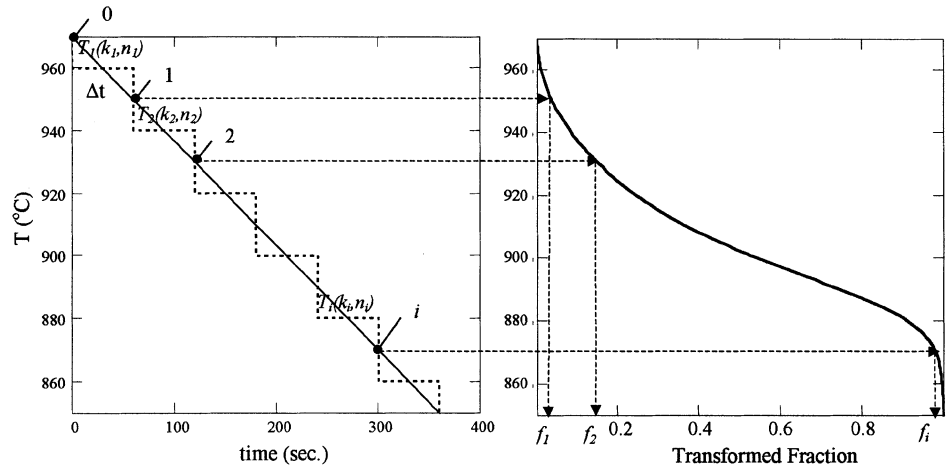

Fig. 7—Schematic diagram, showing the approximation of continuous cooling as the sum of short time isothermal holding.

These calculations present a numerical solution of the "general expression of the concept of additivity" formulated by Cahn.[30,31]

On the basis of the previous description, a computer program was created to derive the optimized JMA kinetic parameters at different temperatures from the DSC experimental results (Figure 8). The input data were the transformed fraction as a function of the temperature for cooling rates of 10 °C, 20 °C, 30 °C, and 40 °C/min. The program contained loops for the kinetic parameters at the different temperature stages (k_1, k_2, and k_i and n_1, n_2, and n_i). The experimental transformed fractions were compared with the calculated fractions, and errors were minimized using a "sum-squared" error technique.

For the calculations (in this particular case, the $\beta \Rightarrow \alpha$ transformation in Ti-6Al-4V), it was accepted that n does not depend on the temperature ($n_1 = n_2 = n_i$). This assumption is valid for most transformations and over appreciable temperature ranges. The value of n depends largely on the growth geometry; therefore, it should change only when this geometry varies.[29] As a result, the output of the program to derive JMA kinetic parameters was $n = 1.13$ and $k = k(T)$ (Figure 9).

The n value is related to and gives information on the geometry of the phase transformation. From the value we obtained, it could be assumed that the preferable nucleation sites are β grain boundaries.[29] This is well known and peculiar to phase transformation during cooling in titanium alloys. This was also confirmed by metallographical examinations at different stages of the $\beta \Rightarrow \alpha$ transformation. Similar n values have recently been reported for the titanium alloys 6-2-4-6, β-CEZ, and 10-2-3.[5] It was found that, for 6-2-4-6, $n = 1$ for the temperature range from the β transus (940 °C) to 240 °C below the β transus, and, for β-CEZ, n was in the range from 1 to 1.2 for the temperature range from the β transus (890 °C) to 290 °C below the β transus.

The value of k for the $\beta \Rightarrow \alpha$ transformation in the Ti-6Al-4V alloy studied was found to vary vastly with temperature (Figure 9). It increased significantly when the temperature decreased from the β transus (1000 °C) to 855 °C. A similar tendency of $k(T)$ has recently been reported for the austenite-pearlite phase transformation in steels.[33] This means that, in the aforementioned temperature range, the nucleation rate controls the overall transformation rate. From the DSC results using a high cooling rate (50 °C/min), there was some evidence of a decrease of k when the temperature decreased below 850 °C. All these observations were in good agreement with the C curves of the TTT diagram for Ti-6Al-4V.[22]

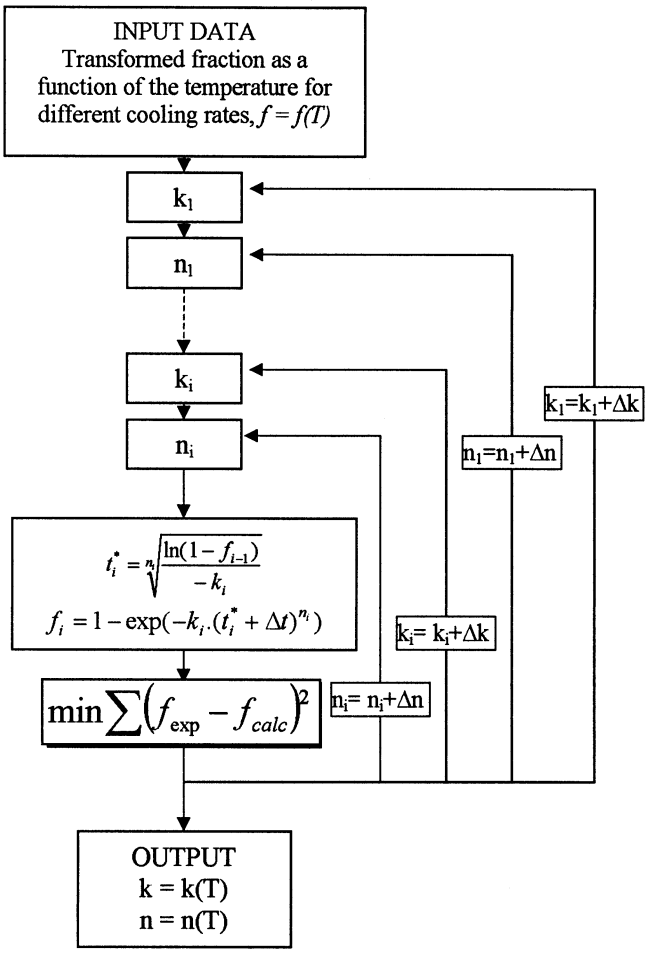

Fig. 8—Flow diagram of program for calculation of JMA kinetics parameters.

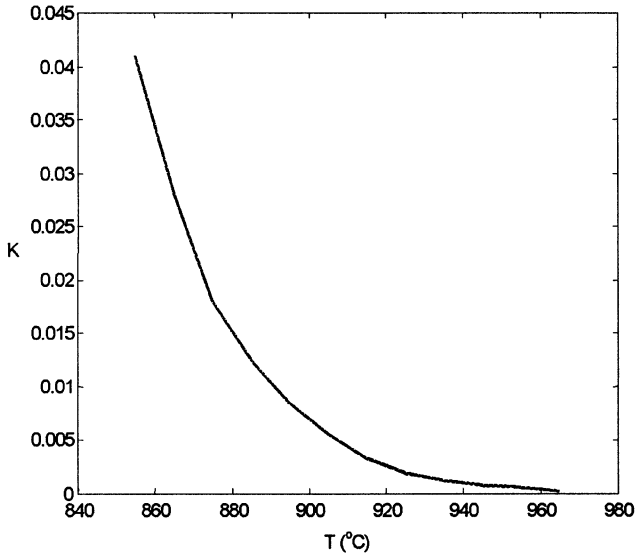

Fig. 9—Calculated rate constant (k) as a function of the temperature for $\beta \Rightarrow \alpha$ transformation in Ti-6Al-4V.

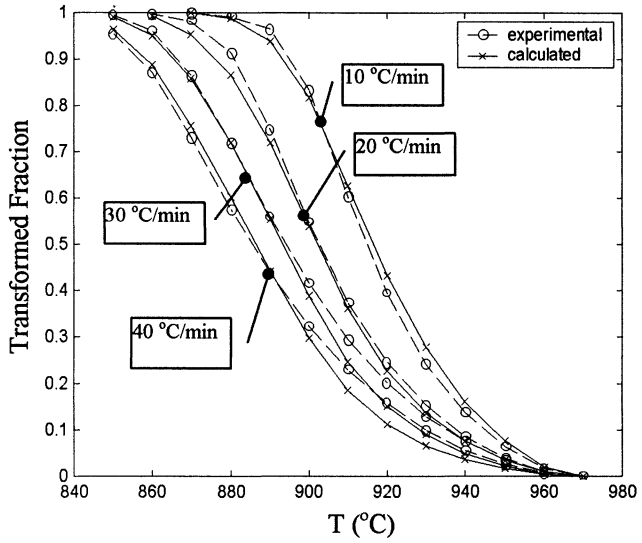

Fig. 10—Experimental and calculated degree of $\beta \Rightarrow \alpha$ transformation in Ti-6Al-4V for different cooling rates.

As the next step in this work, we calculated the transformed fractions for different cooling rates using the derived values of n and k. Good correspondence between the calculated and experimental transformed fraction was found (Figures 10 and 11). There was some deviation, at approximately a 0.05 fraction level, for temperatures above 900 °C and cooling rates above 20 °C/min. The main reason for the deviation at high temperatures was that as stated before, the transformation start was not clearly defined in the DSC curves, and a start temperature of 970 °C was attributed for all cooling rates. Also, the experimental error was larger at higher cooling rates. Nevertheless, the agreement between the experimental and model results is considered to be more than acceptable. This agreement between the experimental and calculated degree of transformation gave us confidence in the obtained JMA kinetic parameters. These parameters

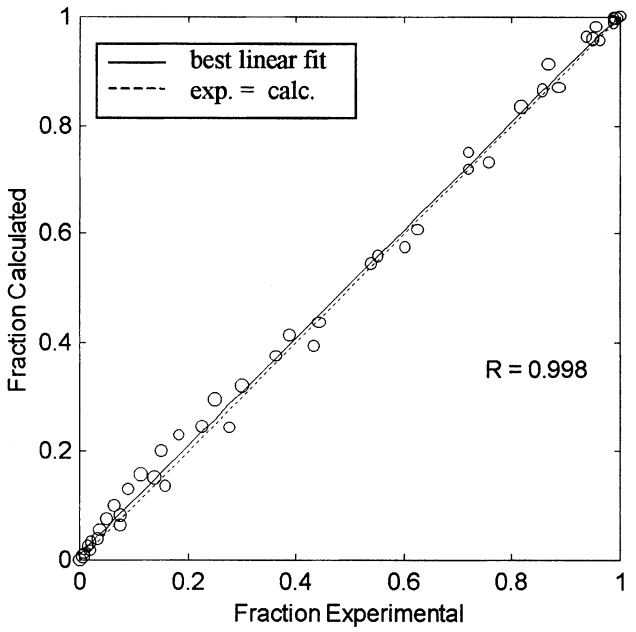

Fig. 11—Regression analysis of calculated and transformed fractions for $\beta \Rightarrow \alpha$ transformation in Ti-6Al-4V. The results are for all cooling rates used.

can be used to trace the course of the $\beta \Rightarrow \alpha$ transformation in a Ti-6Al-4V alloy in real practice, for whatever (not necessarily constant) cooling path.

D. *On Activation Energies of the Transformation*

Integration of the generalized form of the JMA equation (Eq. [3]) for the case of isothermal transformation with nucleation and growth rates independent of time gives

$$f = 1 - \exp(-c' I_V u^m t^n) \qquad [6]$$

where f is the transformed volume fraction at time t, I_v is the nucleation frequency, u is the growth rate, c' is the shape factor, and $m = n - 1$. This equation is actually the JMA law for isothermal transformation and is the same as the well-known form of the JMA equation (Eq. [2]). Taking into account Eqs. [2] and [6], it follows that

$$k = c' I_V u^m \qquad [7]$$

As previously mentioned, both the nucleation and growth rates are described by Arrhenius-type equations. For the nucleation rate,

$$I_V = N_V \frac{k_b T}{h} \exp\left(\frac{-E_N}{RT}\right) = I_{V0} \exp\left(\frac{-E_N}{RT}\right) \qquad [8a]$$

where k_b is the Boltzman constant, h is the Planck constant, N_v is the number density of nucleation sites, E_N is the nucleation activation energy (temperature dependent), and R is the universal gas constant. For the growth rate,

$$u = u_o \exp\left(\frac{-E_G}{RT}\right) \qquad [8b]$$

where E_G is activation energy of growth (temperature independent) and u_o is the growth constant.

Considering Eqs. [7], [8a], and [8b] and the fact that

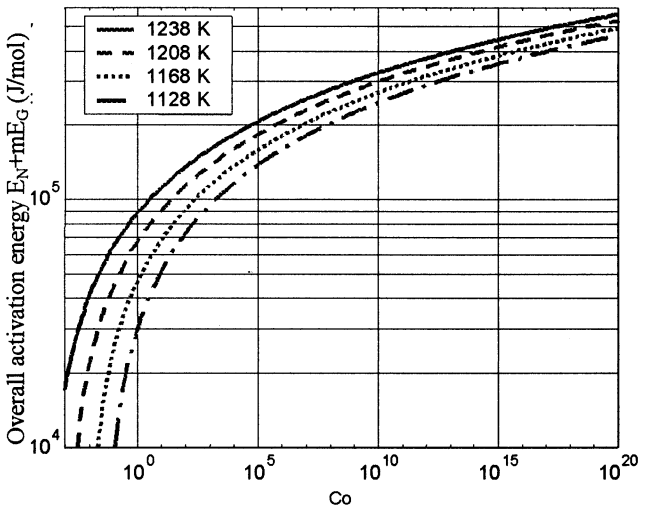

Fig. 12—Overall activation energy for different values of overall rate constant (c_o).

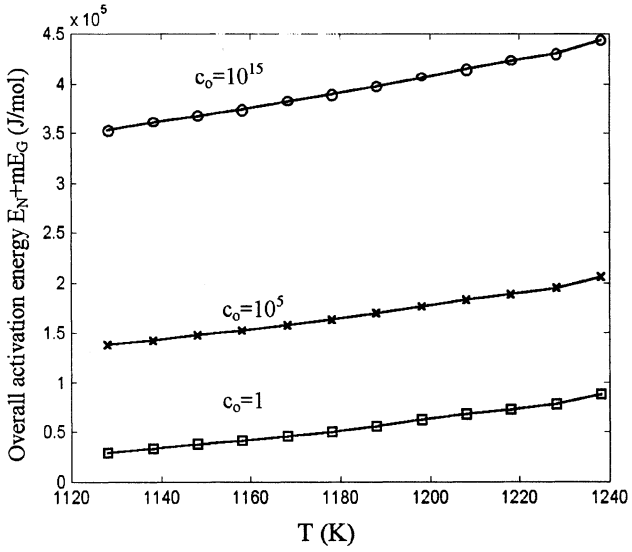

Fig. 13—Overall transformation energy as a function of the temperature assuming different values of the overall transformation constant (c_o).

nucleation activation energy (E_N) is temperature dependent while the activation energy for growth (E_G) is independent of temperature, one can express

$$k(T) = c_o \exp\left(\frac{-(E_N(T) + mE_G)}{RT}\right) = c_o \exp\left(\frac{-E(T)}{RT}\right) \quad [9]$$

where c_o is a new constant ($c_o = c' I v_o u_o^m$), and $E(T)$ is the overall activation energy.

In the previous section, the JMA rate constant for the $\beta \Rightarrow \alpha$ transformation in Ti-6Al-4V as a function of the temperature ($k = k(T)$) was derived (Figure 9). This was still insufficient to solve Eq. [9] and to determine the activation energy as a function of the temperature, since two terms (c_o and $E(T)$) are still unknown. It must be noted here that c_o depends on many factors, such as the shape of the new phase particles, attempt frequency, density of nucleation sites, mechanism of growth, *etc.* Since most of them are difficult to determine, it is impossible to calculate any accurate and reliable value for c_o. Nevertheless, using the previously derived function $k = k(T)$, Eq. [9] was solved graphically in the form given in Figure 12. From such a graph, the function of the activation energy on the temperature can be obtained assuming any value of c_o.

Again, using Eq. [9] and the previously derived function $k = k(T)$, the functional dependence of the activation energy on the temperature was investigated, assuming different values of c_o ($c_o = 1, 10^5$, and 10^{15}) (Figure 13). It is obvious that, for the investigated temperature range, the overall activation energy decreases when the temperature decreases. The function was linear for all c_o values. At high temperatures (>960 °C), there was a trend toward high values. This is reasonable since, from the theory of nucleation at the equilibrium temperature (in this case, β transus = 1000 °C), the nucleation activation energy should be infinity. It should be noted here that the "overall activation energy" is actually the term $E_N(T) + mE_G$. But, since the activation energy of growth is independent of temperature, the previous temperature dependence can be related only to the nucleation activation energy. The term mE_G can be calculated and subtracted using a value of activation energy for growth. Recently, a value of 91 to 98 kJ/mol for the activation energy of growth in Ti-6Al-4V has been reported.[34]

The aforementioned conclusions, in particular, the nucleation activation energy, are consistent with the expected results from the theory of phase transformations.

IV. SUMMARY AND CONCLUSIONS

1. The DSC technique is suitable for a quantitative description of the $\beta \Rightarrow \alpha$ transformation in a Ti-6Al-4V alloy during cooling. Using DSC results, CCT diagrams with lines of isotransformed fraction were proposed.
2. The JMA theory was adapted to describe and model the kinetics of the $\beta \Rightarrow \alpha$ transformation in a Ti-6Al-4V alloy as a function of the temperature. The kinetic parameters of the aforementioned transformation were derived. Using the derived kinetic parameters, the $\beta \Rightarrow \alpha$ transformation in a Ti-6Al-4V alloy can be described for any cooling path and condition.
3. The nucleation rate controls the overall transformation rate of the $\beta \Rightarrow \alpha$ transformation in a Ti-6Al-4V alloy. The nucleation activation energy decreases linearly with decreasing temperature.

ACKNOWLEDGMENTS

This work was carried out within the framework of project "Modelling the Evolution of Microstructure during Processing of Titanium Alloys" sponsored by the UK Engineering and Physical Sciences Research Council under Grant No. GR/M 19932.

REFERENCES

1. R. Boyer, G. Welsch, and E.W. Collings: *Materials Properties Handbook: Titanium Alloys*, ASM INTERNATIONAL, Materials Park, OH, 1994.

2. R.A. Wood and R.J. Favor: *Titanium Alloys Handbook*, Metals and Ceramics Information Center, Batella Publ. No. MCIC-HB02, OH, 1972.
3. *Titanium '95: Science and Technology*, Proc. 8th World Conf. on Titanium, Birmingham, United Kingdom, Oct. 22–26, 1995, P.A. Blenkinsop, W.J. Evans, and H.M. Flower, eds., The Institute of Materials, London, 1996.
4. *Titanium and Titanium Alloys: Scientific and Technological Aspects*, Proc. 3rd Int. Conf. on Titanium, Moscow, May 18–21, 1976, J.C. Williams and A.F. Belov, eds., Plenum Press, New York, NY, 1982.
5. S. Bein and J. Bechet: *J. Phys. IV*, 1996, vol. 6 (C1), pp. 99-108.
6. E. Laude, E. Gautier, and S. Denis: *Titanium '95: Science and Technology*, Proc. 8th World Conf. on Titanium, Birmingham, United Kingdom, Oct. 22–26, 1995, P.A. Blenkinsop, W.J. Evans, and H.M. Flower, eds., The Institute of Materials, London, 1996, pp. 2330-37.
7. M.P. Jackson, M.J. Starink, and R.C. Reed: *Mater. Sci. Eng. A*, 1999, vol. 264, pp. 26-38.
8. J. Vazquez, C. Wagner, P. Villares, and R. Jimenez-Garay: *Acta Mater.*, 1996, vol. 44 (12), pp. 4807-13.
9. A. Borrego and G. Gonzalez-Doncel: *Mater. Sci. Eng. A*, 1998, vol. 245, pp. 10-18.
10. J. Vazquez, P. Villares, and R. Jimenez-Garay: *J. Alloys Compounds*, 1997, vol. 257, pp. 259-65.
11. A. Borrego and G. Gonzalez-Doncel: *Mater. Sci. Eng. A*, 1998, vol. 252, pp. 149-52.
12. M.P. Trujillo, A. Orozco, M. Casas-Ruiz, R.A. Ligero, and R. Jimenez-Garay: *Mater. Lett.*, 1995, vol. 24, pp. 287-90.
13. R. Benedictus, A. Bottger, and E.J. Mittemeijer: *Z. Metallkd.*, 1998, vol. 89, pp. 168-76.
14. J.A. Augus and J.E. Bennett: *J. Thermal Analysis*, 1978, vol. 13, pp. 283-92.
15. M. Avrami: *J. Chem. Phys.*, 1939, vol. 7, p. 1103.
16. M. Avrami: *J. Chem. Phys.*, 1940, vol. 8, p. 212.
17. M. Avrami: *J. Chem. Phys.*, 1941, vol. 9, p. 177.
18. W.A. Johnson and R.F. Mehl: *Trans. Am. Inst. Min. Metall. Eng.*, 1939, vol. 135, p. 416.
19. W. Sha and Z. Guo: *J. Alloys and Compounds*, 1999, vol. 290, p. L3-7.
20. J. Sieniawski, R. Filip, W. Ziaja, and F. Grosman: *Titanium '95: Science and Technology*, Proc. 8th World Conf. on Titanium, Birmingham, United Kingdom, Oct. 22–26, 1995, P.A. Blenkinsop, W.J. Evans, and H.M. Flower, eds., The Institute of Materials, London, 1996, pp. 1411-18.
21. E. Scheil: *Arch Eisenhuttenwes.*, 1935, vol. 12, p. 565.
22. S. Malinov, W. Sha, and Z. Guo: *Mater. Sci. Eng. A*, 2000, vol. 283, pp. 1-10.
23. B.D. Cullity: *Elements of X-ray Diffraction*, Addison-Wesley Series in Metallurgy and Materials, Reading, MA, 1978, pp. 411-13.
24. E.J. Mittemeijer: *J. Mater. Sci.*, 1992, vol. 27, pp. 3977-87.
25. J.S. Jones and H.K.D.H. Bhadeshia: *Metall. Mater. Trans. A*, 1997, vol. 28A, pp. 2005-13.
26. W. Sha and H.K.D.H. Bhadeshia: *Mater. Sci. Eng. A*, 1997, vol. 223, pp. 91-98.
27. J.W. Christian: *The Theory of Transformation in Metals and Alloys: Equilibrium and General Kinetic Theory*, 2nd ed., Pergamon, Oxford, United Kingdom, 1975, pp. 418-75.
28. E.J. Mittemeijer: Max Planck Institute for Metals Research, Stuttgart, Germany, private communication. 1999.
29. J.W. Christian: *The Theory of Transformation in Metals and Alloys: Equilibrium and General Kinetic Theory*, 2nd ed., Pergamon, Oxford, United Kingdom, 1975, pp. 542-46.
30. J.W. Cahn: *Acta Metall.*, 1956, vol. 4, p. 449.
31. J.W. Cahn: *Acta Metall.*, 1956, vol. 4, p. 572.
32. M. Lusk and Herng-Jeng Jou: *Metall. Mater. Trans. A*, 1997, vol. 28A, pp. 287-91.
33. D. Homberg: *Acta. Mater.*, 1996, vol. 44, pp. 4375-85.
34. F.J. Gil and J.A. Planell: *Scripta Metall. Mater.*, 1991, vol. 25, pp. 2843-48.